Mon. Not. R. Astron. Soc. **000**, 1–?? (2010) Printed 5 July 2011 (MN LATEX style file v2.2)

3C390.3: More stable Evidence for Origination of Double-Peaked Broad Balmer Lines from Accretion Disk Near Central Black Hole

Xue-Guang Zhang[1,2⋆]
[1] *Purple Mountain Observatory, Chinese Academy of Sciences, 2 Beijing XiLu, Nanjing, Jiangsu, 210008, P. R. China*
[2] *Department of Physics and Astronomy, Texas A&M University, College Station, Texas, 77843-4242, U.S.A.*

ABSTRACT
In this manuscript, the structure of broad emission line regions (BLRs) of well-mapping double-peaked emitter (AGN with broad double-peaked low-ionization emission lines) 3C390.3 is studied. Besides the best fitted results for double-peaked broad optical balmer lines of 3C390.3 by theoretical disk model, we try to find another way to further confirm the origination of double-peaked line from accretion disk. Based on the long-period observed spectra in optical band around 1995 collected from AGN WATCH project, the theoretical disk parameters of disk-like BLRs supposed by elliptical accretion disk model (Eracleous et al. 1995) have been well determined. Through the theoretical disk-like BLRs, characters of observed light-curves of broad double-peaked Hα of 3C390.3 can be well reproduced based on the reverberation mapping technique. Thus the accretion disk model is preferred as one better model for BLRs of 3C390.3. Furthermore, we can find that different disk parameters should lead to some different results about size of BLRs of 3C390.3 from the one measured through observational data, which indicates the measured disk parameters are significantly valid for 3C390.3. After that, the precession of theoretical elliptical disk-like BLRs being considered, we can find that the expected line profile in 2000 by theoretical model is consistent with the observed line profile by HST around 2000. Based on the results, we can further believe that the origination of broad double-peaked balmer emission lines of 3C390.3 are from accretion disk around central black hole.

Key words: Galaxies:Active – Galaxies:nuclei – Galaxies:Seyfert – quasars:Emission lines – Galaxies:individual: 3C390.3

1 INTRODUCTION

The properties of objects with broad double-peaked low-ionization emission lines (hereafter, double-peaked emitters) have been studied for more than two decades, since the double-peaked emitters were found in nearby radio galaxies (Stauffer et al. 1983, Oke 1987, Perez et al. 1988, Halpern 1990, Chen et al. 1989, Chen & Halpern 1989). Some theoretical models have been proposed to explain the properties of double-peaked broad emission lines which can be used as one probe of the broad-line regions of active galactic nuclei (Eracleous et al. 2009), such as binary black hole model (Begelman et al. 1980, Gaskell 1983, 1996, Boroson & Lauer 2009, Lauer & Boroson 2009, Zhang et al. 2007), double stream model (Zheng et al. 1990, 1991, Vellieux & Zheng 1991), accretion disk model (Chen et al. 1989, Chen & Halpern 1989, Eracleous et al. 1995, 1997, Bachev 1999, Hartnoll & Blackman 2000, 2002, Karas et al. 2001, Gezari et al. 2007, Flohic & Eracleous 2008, Lewis et al. 2010, Tran 2010, Chornock et al. 2010, Gaskell 2010) etc.. Although which theoretical model is more preferred for double-peaked emitters is still an open question, the accretion disk model which indicates double-peaked broad emission lines are from central accretion disk is so far the more widely accepted model applied to explain the properties of double-peaked broad emission lines.

Due to the un-obscured emitting region on the receding jet, the double-stream model can be ruled out for double-peaked emitter 3C390.3 (Livio & Xu 1997). Through the long-period observational results, binary black hole model has also been ruled out due to unreasonable large central BH masses for some double-peaked emitters, such as Arp102B, 3C390.3 (Eracleous et al. 1997). Furthermore, based on the long-period variations of double-peaked broad emission lines, accretion disk model is successfully applied to reproduce the characters of varying observed line profiles

⋆ xgzhang@pmo.ac.cn

of double-peaked emitters, such as the individual double-peaked emitter NGC1097 (Storchi-Bergmann et al. 1995, 1997, 2003), and one sample of double-peaked emitters (Lewis et al. 2010, Gezari et al. 2007). However, we should note that although accretion disk model is so far the widely accepted theoretical model for double-peaked emitters, the other theoretical models can be expected to be preferred for some special double-peaked emitters, such as the x-shaped radio objects which could be candidates for objects with binary black holes in central regions (Merritt & Ekers 2002, Zhang et al. 2007). Thus, only based on the double-peaked appearance of broad emission lines, there is no confirmed way to affirm which theoretical model is more preferred for double-peaked emitter.

Among the sample of double-peaked emitters (Eracleous & Halpern 1994, 2003, Eracleous et al. 1995, Strateva et al. 2003), 3C390.3 is one well studied double-peaked emitter, also one well-studied mapping AGN (Dietrich et al. 1998, O'Brien et al. 1998, Leighly et al. 1997, Shapovalova et al. 2001, 2010, Sergeev et al. 2002, Peterson et al. 2004, Pronik & Sergeev 2007, Sambruna et al. 2009, Jovanovic et al. 2010). Based on the reverberation mapping technique (Blandford & Mckee 1982) and virialization method (Peterson et al. 2004, Collin et al. 2006, Peterson & Bentz 2006, Peterson 2010), size of BLRs (distance between central black hole and broad line emission gas clouds) and central virial BH masses of 3C390.3 have been well determined (Peterson et al. 2004, Onken et al. 2004, Kaspi et al. 2005, Bentz et al. 2006, 2009, Brandon & Bechtold 2007). Besides the common BH masses and size of BLRs, through the theoretical accretion disk model applied for observed double-peaked broad emission lines, some basic disk parameters of supposed theoretical disk-like BLRs of 3C390.3 have also been measured (Eracleous & Halpern 1994), such as the inclination angle of accretion disk, the inner and outer radius of BLRs in accretion disk etc.. However, only due to the best fitted results for double-peaked balmer lines by accretion disk model, we can not firmly confirm that the double-peaked broad emission lines are exactly coming from disk-like BLRs in accretion disk around central black hole for 3C390.3.

Besides the best fitted results for double-peaked broad emission lines by theoretical models, based on the pioneer work by Blandford & Mckee (1982), geometrical structures of BLRs can be mathematically structured by so-called transfer function in the reverberation mapping technique through some special mathematical methods (such as the Maximum Entropy Method, Narayan & Nityananda, 1986) applied to the properties of long-period observational varying both continuum emission and broad line emission (Peterson et al. 1993, 1994, Horne et al. 1991, Goad et al. 1993, Wanders & Horne 1994, Pijpers & Wanders 1994, Krolik 1994, Winge et al. 1995, Bentz et al. 2010). However, it is unfortunate that there should be NOT unique solution to the so-called transfer function used to determine the structures of BLRs of AGN, due to the less complete information about variations of continuum and broad emission lines (Maoz 1996). Thus, even based on the solution of transfer function, the supposed theoretical and mathematical geometrical structures of BLRs of AGN can NOT still be firmly confirmed.

In the previous remarkable work about structures of BLRs of AGN, the main objective is to determine the structures of BLRs through observational properties/characters. However, we think it will be also very interesting to check whether the observational properties of long-period variations of broad line emission and/or continuum emission could be better reproduced through the reverberation mapping technique, based on the expected structures of BLRs supposed by theoretical model, which is the main objective of our paper.

The structures of our paper are as follows. Section 2 gives some information about observed spectra of 3C390.3 around 1995 and how to find theoretical disk parameters for the supposed disk-like BLRs through the best fitted results for broad double-peaked balmer lines by theoretical elliptical accretion disk model (Eracleous et al. 1995). Section 3 shows the results through the reverberation mapping technique under the disk-like BLRs for 3C390.3. Finally section 4 gives some detailed discussions and conclusion. The cosmological parameters $H_0 = 70\mathrm{km}\cdot\mathrm{s}^{-1}\mathrm{Mpc}^{-1}$, $\Omega_\Lambda = 0.7$ and $\Omega_m = 0.3$ have been adopted here.

2 FITTED RESULTS FOR SPECTRA OF 3C390.3 AROUND 1995

As one well mapping double-peaked broad line AGN, 3C390.3 (z=0.056) is one target included in the project of AGN WATCH (http://www.astronomy.ohio-state.edu/~agnwatch/), which is a consortium of astronomers who have studied the inner structure of AGN through continuum and emission-line variability. From the AGN WATCH project, we can collect 133 spectra of 3C390.3 in optical band observed around 1995 by different instruments in different observatories. Meanwhile the light curves of continuum and broad emission lines after corrections of some necessary contamination are also collected from the website. The detailed descriptions about the instruments and techniques for the observed spectra can be found in Dietrich et al. (1998). Here, we do not describe the information any more. We mainly focus on how to determine the disk parameters by theoretical accretion disk model for 3C390.3.

In order to obtain reliable disk parameters for disk-like BLRs of 3C390.3 supposed by the theoretical accretion disk model applied to fit double-peaked broad emission lines, we prefer to use double-peaked broad Hα rather than double-peaked broad Hβ, because of the more apparent double peaks of broad Hα (one peak of double-peaked broad Hβ is mixed by [OIII]$\lambda 4959, 5007\mathring{A}$ doublet) and more stronger broad Hα than broad Hβ. Thus we mainly focus on the 66 out of the 133 observed spectra with reliable broad Hα within rest wavelength from $6200\mathring{A}$ to $7300\mathring{A}$.

There are so far several kinds of accretion disk models which can be applied for double-peaked emitters, circular with/without spiral arms accretion disk model(Chen et al. 1989, Chen & Halpern 1989, Hartnoll & Blackman 2002), elliptical accretion disk model (Eracleous et al. 1995), warped accretion disk model (Hartnoll & Blackman 2000), stochastically perturbed accretion disk model (Flohic & Eracleous 2008) etc.. In this paper, the elliptical accretion disk model (Eracleous et al. 1995) is preferred, because the model can explain most of the observational spectral features of broad double-peaked emission lines (especially fea-

tures for extended asymmetric line wings) with less number of necessary model parameters. Furthermore, the most part of flux density of broad double-peaked line emission is from disk-like BLRs into accretion disk, the existence of arms (Hartnoll & Blackman 2002) and/or warped structures (Hartnoll & Blackman 2000) and/or bright spots (Flohic & Eracleous 2008) are mainly applied for subtle structures of double-peaked line profiles (such as some cusps around the peaks etc.), which have few effects on the results based on Cross Correlation Function in reverberation mapping technique. The detailed description of the elliptical accretion disk model with seven model parameters can be found in Eracleous et al. (1995). The seven necessary parameters are inner radius r_0, out radius r_1, eccentricity of elliptical rings e, local broadening velocity σ, inclination angle of disk-like BLRs i, line emissivity slope ($f_r \propto r^{-q}$) and orientation angle of elliptical rings ϕ_0. Through the Levenberg-Marquardt least-squares minimization method applied to fit the double-peaked broad Hα by elliptical accretion disk model as what we have done for the x-shaped radio source SDSS J1130+0058 (Zhang et al. 2007), the seven disk parameters in elliptical accretion disk model can be well determined. The procedures to determine the disk parameters for BLRs of 3C390.3 are as follows.

First and foremost, in order to check the results from reverberation mapping technique under the structures of BLRs supposed by the accretion disk model, we should measure reliable theoretical disk parameters for disk-like BLRs of 3C390.3. Before starting to fit the observed broad double-peaked Hα, we first check the spectra of 3C390.3 by eye, and find that the spectra marked with 'ce' (corresponding observatory can be found in Table 1 in Dietrich et al. 1998) have some unexpected absorption features around 6500$\mathring{A}$ in rest wavelength. The weird absorption features can not be found in the other spectra observed by instruments in other observatories, which should bring some larger uncertainties in measured disk parameters when broad Hα is fitted by accretion disk model. Thus the absorption features (rest wavelength from 6507$\mathring{A}$ to 6525$\mathring{A}$) in the 24 spectra marked with 'ce' should be rejected, when the broad Hα are fitted by the elliptical accretion disk model for 3C390.3. Besides the weird absorption features in the 24 spectra marked with 'ce', in order to reduce the effects of narrow emission lines ([OI]λ6300, 6363$\mathring{A}$, [NII]λ6548, 6583$\mathring{A}$, [SII]λ6716, 6731$\mathring{A}$ and narrow Hα) in all the spectra, the parts of narrow emission lines are also masked when broad Hα are fitted, rest wavelength from 6268$\mathring{A}$ to 6326$\mathring{A}$ for [OI]λ6300$\mathring{A}$, rest wavelength from 6350$\mathring{A}$ to 6388$\mathring{A}$ for [OI]λ6363$\mathring{A}$, rest wavelength from 6533$\mathring{A}$ to 6619$\mathring{A}$ for [NII]λ6548, 6583$\mathring{A}$ and narrow Hα, rest wavelength from 6703$\mathring{A}$ to 6743$\mathring{A}$ for [SII]λ6716, 6731$\mathring{A}$ (the grey shadows shown in Figure 1, Figure 2 and Figure 5). In other words, only the double-peaked broad component of Hα without weird absorption features and without narrow emission lines are fitted. After the prepared work, the double-peaked broad Hα are fitted two times as follows.

Firstly, the 39 spectra with high quality (more than 280 reliable data points within rest wavelength range from 6160$\mathring{A}$ to 6920$\mathring{A}$) and without unexpected absorption features around 6500$\mathring{A}$ are fitted by the elliptical accretion disk model. Then through the measured disk parameters, the two parameters of eccentricity and inclination angle are firstly determined for the 39 spectra, because eccentricity and inclination angle should not be changed with passage of time. The mean values of the two parameters for the 39 spectra are accepted as the reliable values for the two parameter. Then all the 66 spectra are fitted again by the accretion disk model with the accepted constant inclination angle and eccentricity. Figure 1 shows the best fitted results for some selected broad Hα by elliptical accretion disk model with MJD from 49770 to 50051. In the figure, two spectra with unexpected absorption features (marked with '49860ce' and '49984ce') are also shown, the shadow areas represent the masked ranges for narrow emission lines. Figure 2 shows the corresponding residuals ($y_{obs} - y_{model}$, observed data minus expected model data) for the shown examples in Figure 1. In the figure, shadow areas represent the narrow emission lines, each double horizontal dashed lines represent the range of $[f_0 - 1, f_0 + 1]$, where $f_0 = 0, 10, 20...80$ representing the zero point for each spectrum are shown as solid horizontal line in the figure. The results shown in Figure 2 and in Figure 1 indicate that the elliptical disk model is better for double-peaked broad emission lines of 3C390.3, and further indicate that the probable existing hot spots and/or warped structures have few effects on the measured flux density of broad Hα and few effects on our final results and conclusion, i.e., the hot spots and/or ward structures are weak for observed spectra of 3C390.3 around 1995, and elliptical accretion disk model is efficient and sufficient for 3C390.3 around 1995.

Figure 3 shows the distributions of the seven disk parameters, and the distributions of the parameter of $\log(\chi^2)$ (the value of the summed squared residuals divided by the degree of freedom for the returned model parameter values, which is one parameter as the residual to determine whether the theoretical model is preferred) for the 39 high quality spectra in upper three panels and for all the 66 spectra in the other six panels. The final accepted disk parameters are: inner radius $r_0 = 216 \pm 26 R_G$, outer radius $r_1 = 1263 \pm 70 R_G$, eccentricity $e = 0.13 \pm 0.04$, inclination angle $i = 29.57 \pm 1.67^\circ$, orientation angle $\phi_0 = -23 \pm 7^\circ$, emissivity power slope $q = 1.65 \pm 0.26$ ($f(r) \propto r^{-q}$) and local broadening velocity $\sigma = 742 \pm 145$km/s. Actually, we should note that some of the theoretical disk parameters, r_0, r_1, q, ϕ_0, σ, should depend on the strength of continuum emission, in other words, the parameters are time dependent. However, there need to be long-term progressive changes in the ionizing flux to change these variables. Moreover, from the results shown in Figure 3, we can find that there are tiny variations for these parameters, which indicates that the mean values for the theoretical disk parameters can be used to trace the actual physical disk parameters for 3C390.3 around 1995.

Before proceeding further, we compare our measured disk parameters with the previous results reported in the literature. In the sample of double-peaked emitters from radio galaxies, Eracleous & Halpern (1994) gave the results about disk parameters for BLRs through circular accretion disk model (Chen et al. 1989) for double-peaked broad Hα observed in 1988 for 3C390.3 (simple results can also be found in Figure 6 and in Section 4.5 in Sambruna et al. 2009), which are some different from our results determined through elliptical accretion disk model (Eracleous et al. 1995). We know that in accretion disk model, full width at zero intensity (FWZI) of double-peaked broad emission

lines sensitively depends on inner radius of disk-like BLRs, smaller inner radius leads to broader FWZI. From the fitted results shown in Figure 4 in Eracluous & Halpern (1994), we can find that in order to better fit the broad wings of broad Hα, the inner radius should be some smaller than $380R_G$ (the one listed in Eracluous & Halpern 1994). Thus our inner radius $r_0 = 216R_G$ should be reasonable. Peak separation sensitively depends on the outer radius, thus there are similar results about outer radius in Eracluous & Halpern (1994) and in our paper. In order to better fit the cusp feature around blue peak, the elliptical disk model should be more efficient than the totally symmetric circular disk model, i.e., the parameters of eccentricity and orientation angle should be active. The separation between peak intensity and zero intensity of blue (or red) part of Hα should depends on the emissivity power slope. The larger distance between our inner radius and outer radius indicates that our emissivity slope should be smaller than 3 (the one listed in Eracluous & Halpern 1994). Thus our emissivity slope $q = 1.65$ should be reasonable. Line width of double-peaked broad line sensitively depends on inclination angle, thus it is clear there are similar value about inclination angle $i \sim 30^\circ$ in our paper and in Eracluous & Halpern (1994). Because the elliptical accretion disk model is more efficient for 3C390.3 than the circular accretion disk model, the effects from local broadening velocity should be lower. Thus our local broadening velocity $\sigma \sim 750$km/s smaller than 1900km/s in Eracluous & Halpern (1994) should be reasonable.

Besides the disk parameters, it is interesting to check the variations of line profiles of double-peaked broad Hα. As shown in Veilleux & Zheng (1991), there are significant variations of relative flux ratio of the two peaks within the period from 1974 to 1988. Certainly, the variations can not be successfully explained by the elliptical accretion disk model, because the disk precession period of 3C390.3 based on the elliptical accretion disk model is about several hundreds of years as we should discuss in the following. However, during the period (about 500days) around 1995 included in AGN WATCH project, the variations of flux ratio of the two peaks are tiny as shown in Figure 4. In the figure, two kinds of flux ratios are shown, the one with mean value of 1.01 ± 0.02 (0.02 is standard deviation for the mean value) is the ratio of the blue part to red part of broad Hα divided by $6564.61\mathring{A}$ (the theoretical center wavelength of Hα), the other one with mean value of 1.46 ± 0.06 (0.06 is standard deviation) is the intensity ratio of the blue peak to red peak. Similar results for 3390.3 around 1995 can also be found in Dietrich et al. (1998). The more recent results about the flux ratio of the two peaks of 3C390.3 from 1995 to 2007 can be found in Shapovalova et al. (2010), there are tiny variations of the flux ratio of the two peaks in the 5years period as shown in Figure 13 in Shapovalova et al. (2010). Due to the tiny variations, we believe that there are tiny variations for disk parameters obtained from the observed spectra during 1995, and that is the reason why we select the spectra observed around 1995. In other words, the structures of BLRs of 3C390.3 are stable around 1995, which re-confirm that there are tiny variations of disk parameters shown in Figure 3.

Last but not least, we should note the collected 66 spectra in optical band for 3C390.3 are the observed spectra before the intercaliberation method (Van Groningen & Wanders 1992) applied to consider the effects from different observational instruments in different configurations as discussed in Dietrich et al. (1998). In this paper, we mainly focus on the disk parameters, rather than the flux densities of broad Hα which should be directly collected from AGN WATCH project with contamination being corrected. The main effect from intercaliberation method on the corrected line profile is the broadening velocity in the method. However, the broadening velocity is only about tens of kilometers per second when intercaliberation method is applied, which is much smaller than line width of broad Hα. Thus, the effects from intercaliberation method on the measured disk parameters through elliptical accretion disk model can be totally ignored.

Before to finish the section, we consider the following question whether there are other values for disk parameters in the disk model applied to well fit observed double-peaked broad Hα. In other words, the question is whether the solutions to the disk parameters are unique. If the answer is yes, there should be one set of values for the disk parameters in the following mathematical procedure, and we will try to determine whether our mathematical procedure can be applied to determine the available parameter space. If the answer is no, the following mathematical procedure should be simple and succinct. To give one precise mathematical solution to the question is very difficult. We consider the question as follows. The observed double-peaked broad Hα is re-fitted. When procedure starts to fit line profile, one of the disk parameters is fixed to one value much different from the accepted value above (half of the accepted value for the parameter), and the other disk parameters with the same starting values in fitting procedure are free. Then the Levenberg-Marquardt least-squares minimization technique is applied to find the best fitted results for observed double-peaked broad Hα and find the best solutions for the disk parameters. Actually, the software package MPFIT in Markwardt IDL Library (http://www.physics.wisc.edu/∼craigm/idl/) is used to perform the least-squares fitting and to find the best solution. In order to clearly compare the fitted results for different disk parameters, the value $flux_{fit1-fit2}$ is calculated, where $fit2$ means the best fitted results for accepted disk parameters shown in Figure 3 and $fit1$ means the best fitted results for one fixed disk parameter with half of the accepted value for the parameter. Figure 5 shows the fitted results, and the corresponding values of $flux_{fit1-fit2}$. The apparent and large difference (residual to some extent) between $fit1$ and $fit2$ indicates that solutions to disk parameters based on accretion disk model are unique to some extent. Thus, in the following mathematical procedure to determine geometrical structure of emission line regions, there are fixed disk parameters.

Based on the results above, through the disk parameters, one kind disk-like geometrical structures of BLRs of 3C390.3 can be well structured. Then it is very interesting to check whether the characters of observed light-curves can be reproduced through the theoretical disk-like BLRs of 3C390.3, which is the main objective of the following section.

3 RESULTS ABOUT REVERBERATION MAPPING TECHNIQUE UNDER ELLIPTICAL ACCRETION DISK MODEL

In the section above, one kind geometric structure of BLRs of 3C390.3 have been supposed by the theoretical elliptical accretion disk model (Eracleous et al. 1995). In this section, we will mainly check whether the supposed disk-like BLRs are valid to reproduce properties of observed continuum and broad line variability, through reverberation mapping technique.

In order to clearly build one physical geometrical structure of disk-like BLRs, the length of one gravitational radius (R_G) in physical unit should be firstly determined, i.e., it is necessary to determine the masses of central black hole of 3C390.3. Here the BH masses of 3C390.3, $M_{BH} = 4.68 \times 10^8 \mathrm{M}_\odot$, is accepted. For 3C390.3, the two kinds of BH masses, both virial BH masses (Peterson et al. 2004) and BH masses from M-sigma relation (Tremaine et al. 2002, Ferrarese & Merritt 2001, Gebhardt et al., 2000, Gültekin et al. 2009, Woo et al. 2010, Lewis & Eracleous 2006) can be found in literature, which are similar. Thus we do not worry about the accuracy of BH masses of 3C390.3, and accept $R_G \sim 0.0263\mathrm{light} - \mathrm{days}$ based on the BH masses. Through the disk parameters above, it is not difficult to build the physical geometry of the BLRs of 3C390.3 supposed by theoretical model. Then it is interesting to check the results based on the reverberation mapping technique through the supposed disk-like BLRs as follows.

First and Foremost, we accept the assumptions listed in Peterson (1993) for reverberation mapping technique, 1): the continuum emission is from one central source which is much smaller than BLRs. The assumption is efficient for 3C390.3, although double-peaked broad line of 3C390.3 is assumed from accretion disk. The reported size of BLRs of 3C390.3, the time lag between observed optical balmer emission and observed UV X-ray emission, is about 20 ± 8 light-days (Dietrich et al. 1998, Bentz et al. 2009), i.e., $R_{BLRs} \sim 400 - 1000\mathrm{R_G}$, through cross correlation function method. Based on the theoretical disk parameters for 3C390.3, the flux weighted mean size of BLRs is about $567\mathrm{R_G}$ (simply calculated by $(r_0 + r_1)/(1. + q)$, $q \sim 1.65$ is the line emissivity slope). The result indicates the UV emission region is much near to central black hole, which clearly can be treated as one point source. 2): both continuum emission and line emission are freely and isotopically propagating in the central volume, which can be confirmed by the small covering factor estimated by the appearance of no-absorption features around broad Hα. 3): the line emissions are in rapid response to ionizing continuum, which can be confirmed by the strong correlation between line luminosity and continuum luminosity found by Greene & Ho (2005) and by the much shorter recombination time (about one hundred seconds for standard BLRs) of balmer emission lines and much longer dynamic time (about several years for standard BLRs) than the light travel time across BLRs, as discussed in Peterson (1993).

Besides, we structure the supposed theoretical structures of BLRs of 3C390.3 as follows. More than 10^4 tiny clouds (or so-called test particles, if we treat each tiny cloud with sufficient tiny size) are set in the N elliptical rings (the BLRs), each tiny cloud has its position (radius r and orientation angle ϕ) and line intensity (f). The position in one elliptical ring for one tiny cloudy is created by,

$$\begin{aligned} \phi &\in [0, 2 \times \pi] \\ r &= \frac{r_\star \times (1+e)}{1 - e \times \cos(\phi)} \end{aligned} \tag{1}$$

where $r_0 \leqslant r_\star \leqslant r_1$ and e are the pericenter distance and eccentricity of the disk-like BLRs of 3C390.3, r is the distance from the tiny cloud to the central black hole. From inner boundary r_0 to outer boundary r_1, the pericenter distance for the elliptical rings is evenly separated into N bins, $\log(r_0) \leqslant \log(r_{\star,i}(i = 1 \ldots N)) \leqslant \log(r_1)$ with step of $(\log(r_1) - \log(r_0))/(N-1)$. Because most part of line emission is from inner area of BLRs, thus the parameter of logarithm of pericenter distance ($\log(r)$) is evenly separated, rather than the parameter of pericenter distance (r), which provides more areas in inner part of BLRs. After that, the orientation angle ϕ is evenly separated into M bins, $0 \leqslant \phi_j (j = 1 \ldots M) \leqslant 2 \times \pi$ with step of $2 \times \pi/(M-1)$. Based on the $r_{\star,i}$ and ϕ_j, the supposed theoretical disk-like BLRs can be separated into $(N-1) \times (M-1)$ tiny areas ($A_{i,j}(i = 1 \ldots N, j = 1 \ldots M)$). As long as N is larger enough, the ionizing photo propagating time through each tiny area can be ignored, and each tiny cloud can be simply treated as one point source. The line intensity from each area $f_{i,j}(i = 1 \ldots N, j = 1 \ldots M)$ can be directly calculated by elliptical accretion disk model, and the total line intensity F is the sum of $f_{i,j}$,

$$\begin{aligned} f_{i,j} &= \int_{r_{\star,i}}^{r_{\star,i+1}} \int_{\phi_j}^{\phi_{j+1}} H(model) dr d\phi \propto P(r_i, \phi_j) \\ \sum_j f_{i,j} &= F_i \propto r_{\star,i}^{q_\star} \\ \sum_i \sum_j f_{i,j} &= F \end{aligned} \tag{2}$$

where $H(model)$ is the integrand function used for accretion disk model as shown in Eracleous et al. (1995), $q_\star$ is different from the emissivity slope in elliptical accretion disk model (however if the radius of each bin is uniformly created, then $q_\star \sim 1.0 - q$ as shown in Figure 6), $P(r_i, \phi_j)$ is the function depending on radius and orientation angle to calculate the line intensity of each tiny cloud in the ith elliptical ring which can also be found in Figure 6, F_i and F mean the line intensity from the ith elliptical ring and the total line intensity from total area. Here, we select $N = 60$ and $M = 400$. $N = 60$ confirms that the light travel time from the i bin to $i+1$ bin is much less than 1 day (especially for the bins in inner part of BLRs), the standard date separation of our input light curve of continuum emission. Furthermore, we should note that in our procedure, the listed disk parameters above are taken as fixed values, based on the following considerations. On the one hand, there are tiny variations of line profiles of double-peaked Hα observed around 1995. Based on the observed Hα selected rom AGNWATCH, it is very difficult to find one reliable correlation between line profile variability and disk parameters (especially orientation angle ϕ) through theoretical disk model. In other words, there is no information about the function of $\phi(t)$ where t is date and time. On the other hand, the fixed disk parameters through

tiny varied line profiles around 1995 lead to much simple mathematical procedure.

Figure 6 shows the procedures above to build the structures of BLRs of 3C390.3 based on the disk parameters, including the properties of equation (2). Once the tiny cloud meet the ionizing photo from central source, the line intensity of the tiny cloud is changed immediately as,

$$f_{i,j}(t) \propto f_{i,j}(t-1) \times (\frac{con_{i,j}(t)}{con_{i,j}(t-1)})^{\alpha} \qquad (3)$$

where t is the date with uniform separation of 1 day as discussed below, α is slope of the the corresponding correlation between luminosity of Hα and continuum luminosity, $f_{i,j}$ and $con_{i,j}$ mean the line intensity from area $A(i,j)$ and arriving continuum emission for area $A(i,j)$. For AGN, α is the about 1 for QSOs in Greene & Ho (2005), and for low luminosity AGN in Zhang et al. (2008). However, $\alpha \sim 1$ is not preferred for 3C390.3, Figure 7 shows the correlation between continuum luminosity at $5177\mathring{A}$ and luminosity of broad Hα for the spectra observed around 1995. The values of luminosity of broad Hα and continuum luminosity at $5177\mathring{A}$ are collected from AGN WATCH, the contamination has been corrected. The spearman rank correlation coefficient is about 0.66 with $P_{null} \sim 10^{-9}$. Through the Levenberg-Marquardt least-squares minimization technique, the best weighted fitted result for the correlation can be calculated,

$$L_{H\alpha} = 8.92 \times 10^{42} (\frac{L_{con(5177\mathring{A})}}{10^{44}\mathrm{erg/s}})^{0.26\pm0.03}\mathrm{erg/s} \qquad (4)$$

Thus, we accept $\alpha \sim 0.26$, not ~ 1. Actually, the different index of line-continuum luminosity correlation is due to the contamination of narrow lines around Hα. As shown in Dietrich et al. (1998), the flux density of broad Hα includes contributions from narrow lines around Hα, and flux densities of narrow emission lines are constant for 3C390.3. If we define factor k as flux ratio of pure broad Hα to narrow lines, we should find that points with lower luminosity of Hα in Figure 7 have smaller values of k, points with larger luminosity of Hα in Figure 7 have larger values of k. If the contributions of narrow emission lines are corrected, the index for the correlation shown in Figure 7 should be steeper than 0.26 and near to 1.

Figure 8 shows one simple output line curve of broad Hα based on one test input light curve of continuum emission described by one delta function through the disk-like BLRs determined elliptical accretion disk model for 3C390.3. Because of the extended BLRs, the delta function is delayed and expanded. Light traveling from the central black hole (we assume that the ionizing photos are from central point) to the innerest boundary of the BLRs is about 5days, from the inner boundary ($\sim 216R_G$) to the point with longest distance ($\sim 1640R_G$, larger than the pericenter distance $1263R_G$ for the out boundary, because the BLRs are elliptical disk-like) from central black hole is about 39 days. Thus in the figure, it is clear that 5 days after the burst of continuum, the line intensity starts to vary, and then 39 days after the burst of continuum emission, the variation of line intensity ends. Because the inner part of BLRs emits most of the line intensity of broad Hα, thus the line intensity of total Hα is changed from strong to weak with passage of time as shown in the figure. Furthermore, it should be interesting to check the effects of different geometrical structure on the response output broad Hα, although we have accepted there are fixed and stable disk parameters in section above. We accepted the disk parameters for 3C390.3 under the stochastically perturbed accretion disk model in Flohic & Eracleous (2008, one circular disk part with bright spots), $r_0 = 450R_G$, $r_1 = 1400R_G$, $\sigma = 1300$km/s, $i = 27^o$ and $q = 3$, in spite of the not well fitted results for line profiles with these parameters (not good fitted results for broad wings). Under the model, the output Hα is also shown in Figure 8, It is clear that the response to input continuum described delta function is much different for elliptical disk structure and for circular disk structure. The different response for different geometrical structures indicates the different structures of BLRs of AGN should be discriminated through the light curves of continuum emission and broad emission lines emission, especially when there are HOMOGENEOUS and COMPLETE information for the light curves. Actually, based on the observed light curves of 3C390.3 selected from AGN WATCH project, there is no way to discriminate different geometrical structures of BLRs as what we have shown in the following results. The results shown in the figure indicate that our procedures above DO work, and effects of extended disk-like BLRs on light curve of emission line can be clearly described by our procedures.

Last but not least, the observed light curve of continuum emission at $\sim 5177\mathring{A}$ collected from AGN WATCH is used as the input light curve of continuum emission. The detailed description about the light curve can be found in Dietrich et al. (1998). There are 70 data points included in the light curve from MJD2449517 to MJD2450068. We first create one new light curve of continuum emission with date separation of 1day by linear interpolation method applied to observed light curve of continuum. Then we check the expected output light curve of broad Hα under the supposed elliptical disk-like BLRs. The results are shown in bottom-left panel of Figure 9. It is clear that the expected output light curve of broad Hα is consistent with the observed light curve of broad Hα, the linear correlation coefficient for the correlation between output light curve of Hα and observed light curve of Hα is about 0.85 with $P_{null} \sim 0$. Then through the input light curve of continuum and the output corresponding light curve of broad Hα, it is interesting to estimate the size of BLRs by so-called cross correlation function (CCF). Here, the common interpolated cross-correlation function (ICCF) (Gaskell & Sparke 1986, Gaskell & Peterson 1987, Peterson 1993) is applied to quantify time lag between continuum emission and broad lines emission. We do not consider the z-transfer discrete correlation function (ZDCF, Alexander 1997, Edelson & Krolik 1988, White & Peterson 1994) any more, because results from ZDCF are excellent agreement with the results from ICCF (Peterson et al. 1991, 1992, 2004, Kaspi et al. 2000, Bentz et al. 2010). Furthermore, the corresponding results based on the disk parameters shown in Flohic & Eracleous (2008) are also calculated, and shown in Figure 9. It is clear that although the example shown in Figure 8 indicates the information from light curves can be used to confirm which structure should be more preferred, there is no way to find enough evidence to determine which structure (elliptical disk-like BLRs or circular disk-like BLRs) is preferred, due to the incomplete and in-homogeneous information provided from the observed light curves. Thus, we

mainly compare the calculated time lags between continuum emission and broad line emission, under the two structures.

Figure 9 shows the CCF results from input light curve of continuum and the output light curve of broad Hα, the distribution of the size of BLRs through bootstrap method (a common Monte-Carlo method to estimate the uncertainty of parameter, Press et al. 1992, Peterson et al. 1998). Detailed descriptions about CCF method to estimate size of BLRs (time lag between line emission and continuum emission) and bootstrap method to estimate uncertainties of measured time lag can be found in Peterson (1993). From the results shown in the figure, we can find that the estimated size of BLRs through the input light curve of continuum emission and output light curve of broad Hα under elliptical accretion disk model is also well consistent with the one estimated by the observed light curves of continuum emission and broad line emission, $R_{BLRs} \sim 16.8 \pm 2.1 \mathrm{light}-\mathrm{days}$. We should note that the size of BLRs is the distance from broad Hα emission line region to optical continuum emission region, thus the value is some smaller than $\sim 20 \mathrm{light}-\mathrm{days}$ estimated by the CCF function from light curve of broad Hα and light curve of x-ray/UV emission shown in Dietrich et al. (1998), Bentz et al. (2009) etc., because there are probable 5days lag between optical continuum emission and x-ray emission (Dietrich et al. 1998). Certainly, we also calculate the results based on the circular disk model shown in Flohic & Eracleous (2008), which should be some different from the results for elliptical accretion disk $R_{BLRs} \sim 18.4 \pm 2.1 \mathrm{light}-\mathrm{days}$. However, there is no enough evidence to against the circular disk-like BLRs for 3C390.3, besides the best fitted results for observed line profiles. If there should homogeneous and complete observed light curves, the clear final decision should be given.

In order to further confirm that the disk-like BLRs determined by elliptical accretion disk model is reliable for double-peaked emitter 3C390.3, we also check the CCF results for disk-like BLRs with different disk parameters, in spite of the best fitted results for observed double-peaked broad balmer line. Figure 10 shows the effects of disk parameters on the measured size of BLRs through input continuum emission and output Hα emission based on the elliptical accretion disk model as what we have done above. It is clear that inner radius and emissivity power are the two main parameters which have apparent effects on the theoretically measured size of BLRs of 3C390.3. In the figure, we only show the effects from inner radius, emissivity power, eccentricity and inclination angle of disk-like BLRs, because there are few effects from the other disk parameters. Certainly, more reliable evidence to determine and confirm model parameters should depend on future more detailed and homogeneous observed light curves of continuum emission and broad line emission. The results indicate that the measured disk parameters for BLRs of 3C390.3 are reliable to some extent, and different geometrical structures of BLRs based on different disk parameters should lead to different theoretically measured size of BLRs from size of BLRs through observational results.

The results above indicate that the elliptical accretion disk model can be applied to best fit the observed spectra, i.e., the model can provide fine velocity structures for BLRs of 3C390.3. Furthermore, the elliptical accretion disk model can provide fine geometrical structures which can be applied to reproduce characters of observed light curve of broad Hα. Thus elliptical accretion disk model which can be applied to fit characters of line profiles and variations of broad double-peaked Hα is appropriate to double-peaked emitter 3C390.3.

4 DISCUSSION AND CONCLUSION

As one well-known double-peaked emitter, based on the disk parameters measured above, to check the expected line profile of double-peaked broad balmer emission line of 3C390.3 in different years/periods is very interesting. Although the more recent observed line profiles of double-peaked broad Hα of 3C390.3 in Jan. 2007 can be found in Shapovalova et al. (2010), the observed spectrum in Sep. 2000 by HST STIS is collected, because the reduced spectrum in 2000 is public and conveniently collected from the website of Multimission Archive at STScI (MAST) (http://archive.stsci.edu/) (HST Proposal 8700, PI: Prof. Andre Martel in Space Telescope Science Institute). The detailed description about observational technique for the spectrum around 2000 by HST can be found in Popovic (2003). Here, we mainly check whether the observed line profile of broad balmer emission lines in 2000 can be reproduced through theoretical elliptical accretion disk model based on the disk parameters measured from spectra observed around 1995 for double-peaked emitter 3C390.3.

Before proceeding further, the precession period should be determined. Through the obtained disk parameters, the relativistic precession period of the elliptical disk-like BLRs around central black hole of 3C390.3 can be simply calculated (Weinberg 1972),

$$\begin{aligned} T_{pre} &= \frac{2\times\pi}{\delta_\phi} \sim \frac{2\times\pi}{\frac{6\pi\times G\times M_{BH}}{c^2 A(1-e^2)}} \\ &\sim 70\mathrm{years} \quad (\mathrm{inner\ \ radius}) \\ &\sim 370\mathrm{years} \quad (\mathrm{outer\ \ radius}) \end{aligned} \tag{5}$$

where 'A' is the semi-major axis length and e is the eccentricity. Although, the precession period for outer elliptical rings is very long, the short precession period for inner elliptical rings should lead to some apparent variations of double-peaked broad emission lines from 1995 to 2000.

We simply assume that orientation angle is the unique parameter to vary from 1995 to 2000 in the elliptical accretion disk model. As what we have done in section 3, the elliptical disk-like BLRs are separated into 60 rings. It is clear that orientation angle of each ring in 2000 should be some different due to different semi-major axis length for each ring, $\phi_{2000,i} = \phi_{1995,i} \pm 2\times\pi\times\frac{5}{T_{pre,i}}$, where $\pm$ means the rotating direction of disk-like BLRs is clockwise or anticlockwise for observer. After the orientation angles of the 60 rings around 2000 are determined, line profile expected in 2000 can be re-constructed by the sum of 60 expected double-peaked components from 60 rings, as what we have done in Section 3. Here the theoretical line profile in 2000 is mainly based on the mean spectrum around 1995 in AGN WATCH project. The mean observed spectrum shown as thin solid line in Figure 11 is created by PCA (Principal Components Analysis, so-called Karhunen-Loeve Transform) method applied for all the 66

observed spectra of broad Hα around 1995. The convenient and public IDL PCA program 'pca_solve.pro' written by D. Schlegel in Princeton University is used, which is included in the SDSS software package of IDLSPEC2D (http://spectro.princeton.edu/). Commonly, the first principal component represents the mean spectrum. From the mean spectrum, it is clear that there are similar flux ratio (~ 1.46) of blue peak to red peak of broad double-peaked Hα and similar flux ratio (~ 1) of blue part to red part with those mean values shown in Figure 4.

Figure 11 shows the probable observed line profile of broad double-peaked Hα of 3C390.3 around 2000, and shows the comparison between the mean observed spectrum around 1995 and observed spectrum around 2000. Based on the theoretical accretion disk model, through the results shown in top-left panel in Figure 11, we can find that due to precession period, after about 5 years, the flux ratio of red peak to blue peak should be changed. In the figure, flux density at blue peaks of all the line profiles have been normalized to 1. If rotating direction of disk-like BLRs is clockwise to observer, the expected flux ratio (1.36) of red peak to blue peak of spectrum around 2000 should be smaller than the one (1.46) of observed spectrum around 1995. If rotating direction of disk-like BLRs is anticlockwise to observer, the expected flux ratio (1.68) in 2000 should be larger than the one (1.46) in 1995. Through the observed spectrum in 2000, the flux ratio of blue peak to red peak is about 1.79 ± 0.18. Thus, if anticlockwise rotating disk-like BLRs are applied for 3C390.3, the variations in observed spectra in different years can be naturally explained, although the applied model is over-simplified. The some larger value 1.79 than theoretical expected 1.68 are perhaps due to the not so accurate precession period, the probable existence of varying of hot spots and/or warped structures, different local broadening velocity (which should lead the part around red peak to be some flat), etc.. The not so consistent red peak positions for spectrum around 2000 and mean spectrum around 1995 is probable due to the variation of emissivity power slope during the 5 years from 1995 to 2000.

Finally, a simple summary is listed as follows. Based on the observed spectra around 1995 for 3C390.3, the elliptical accretion disk model is applied to fit the observed double-peaked broad Hα collected from AGN WATCH project. Then based on the disk parameters, the formed geometrical structures of BLRs of 3C390.3 are applied to check the reverberation mapping results for 3C390.3. The disk-like BLRs supposed by theoretical elliptical accretion disk model can well re-produce the observational results about reverberation mapping technique. Thus the disk-like BLRs are preferred for 3C390.3. Furthermore, we check the effects of precession of elliptical disk-like BLRs on the observed line profile. After about 5 years, the line profile of broad double-peaked Hα observed in 2000 by HST can be well expected by the theoretical elliptical accretion disk model, based on the disk parameters measured through spectra observed around 1995, which confirms the elliptical accretion disk model is appropriate to double-peaked emitter 3C390.3 .

ACKNOWLEDGEMENTS

ZXG gratefully acknowledge the anonymous referee for giving us constructive comments and suggestions to greatly improve our paper. ZXG gratefully acknowledges finance support from Chinese grant NSFC-11003034, and the useful discussions from Prof. Ting-Gui Wang in USTC. We thank the project of AGN WATCH (http://www.astronomy.ohio-state.edu/~agnwatch/) to make us conveniently collect spectra of 3C390.3. We thank Prof. Andre Martel in Space Telescope Science Institute who provide public HST spectra of 3C390.3. We thank for the The Multimission Archive at STScI which is a NASA funded project to support and provide to the astronomical community a variety of astronomical data archives, with the primary focus on scientifically related data sets in the optical, ultraviolet, and near-infrared parts of the spectrum. We thank for the public SDSS IDL code provided by Dr. David Schlegel in Princeton University, and the public Markwardt IDL Library. This research has made use of the NASA/IPAC Extragalactic Database (NED) which is operated by the Jet Propulsion Laboratory, California Institute of Technology, under contract with the National Aeronautics and Space Administration.

REFERENCES

Alexander T. 1997, in Astronomical Time Series, ed. D. Maoz, A. Sternberg, & E. M. Leibowitz (Dordrecht: Kluwer), 163
Bachev, R., 1999, A&A, 348, 71
Begelman M. C., Blandford R. D. & Rees M. J., 1980, Nature, 287, 307
Bentz M. C., Peterson B. M., Pogge R. W., Vestergaard M., Onken C. A., 2006, ApJ, 644, 133
Bentz M. C., Peterson B. M., Netzer H., Pogge R. W., Vestergaard M., 2009, ApJ, 697, 160
Bentz M. C., Horne K., Barth A. J., Bennert V. N., Canalizo G., et al., 2010, ApJ, 720, L46
Blandford R. D. & Mckee C. F., 1982, ApJ, 255, 419
Boroson T. A. & Lauer T. R., 2009, Nature, 458, 53
Brandon C. K. & Bechtold J., 2007, ApJS, 168, 1
Chen K. Y. & Halpern J. P., 1989, ApJ, 344, 115
Chen K. Y., Halpern J. P. & Filippenko A. V., 1989, ApJ, 339, 742
Chornock R., Bloom J. S., Cenko S. B., Filippenko A. V., Silverman J. M., Hicks M. D., Lawrence K. J., Mendez A. J., Rafelski M., Wolfe, A. M., 2010, ApJ, 709, 39
Collin S., Kawaguchi T., Peterson B. M., Vestergaard M., 2006, A&A, 456, 75
Dietrich M., Peterson B. M., Albrecht P., Altmann M., Barth A. J., et al., 1998, ApJS, 115, 185
Edelson R. A. & Krolik J. H., 1988, ApJ, 333, 646
Eracleous M. & Halpern J. P., 1994, ApJS, 90, 1
Eracleous M., Livio M., Halpern J. P., Storchi-Bergmann T., 1995, ApJ, 438, 610
Eracleous M., Halpern J. P., Gilbert A. M., Newman J. A., Filippenko A. V., 1997, ApJ, 490, 216
Eracleous M. & Halpern J. P., 2003, ApJ, 599, 886
Eracleous M., Lewis K. T., Flohic H. M. L. G., 2009, NewAR, 53, 133
Ferrarese L. & Merritt D., 2001, MNRAS, 320, L30
Flohic H. M. L. G. & Eracleous M., 2008, ApJ, 686, 138
Gaskell C. M., 1983, N: Quasars and gravitational lenses; Proceedings of the Twenty-fourth Liege International Astrophysical Colloquium, Cointe-Ougree, Belgium, June 21-24, 1983

(A85-13301 03-90). Cointe-Ougree, Belgium, Universite de Liege, 1983, p. 473-477. Sponsorship: Science and Engineering Research Council of England.
Gaskell C. M. & Sparke L. S., 1986, ApJ, 305, 175
Gaskell C. M. & Peterson B. ., 1987, ApJS, 65, 1
Gaskell M., 1996, ApJ, 464, 107
Gaskell C. M., 2010, Nature, 463, 1
Gebhardt K., Bender R., Bower G., Dressler A., Faber S. M., et al., 2000, ApJ, 439, L13
Gezari S., Halpern J. P., Eracleous M., 2007, ApJ, 169, 167
Goad M. R., O'Brien P. T., Gondhalekar P. M., 1993, MNRAS, 263, 149
Greene J. E. & Ho L. C., 2005, ApJ, 630, 122
Gültekin K., Richstone D. O., Gebhardt K., Lauer T. R., Tremaine S., et al., 2009, ApJ, 698, 198
Halpern J. P., 1990, ApJ, 365, L51
Hartnoll S. A. & Blackman E. G., 2000, MNRAS, 317, 880
Hartnoll S. A. & Blackman E. G., 2002, MNRAS, 332, L1
Horne K., Welsh W. F., Peterson B. M., 1991, ApJ, 367, L5
Jovanovic P., Popovic L. C., Stalevski M., Shapovalova A. I., 2010, ApJ, 718, 168
Karas V., Martocchia A. & Subr L., 2001, PASJ, 53, 189
Kaspi S., Smith P. S., Netzer H., Maoz D., Jannuzi B. T., Giveon U., 2000, ApJ, 533, 631
Kaspi S., Maoz D., Netzer H., Peterson B. M., Vestergaard M., Jannuzi B. T., 2005, ApJ, 629, 61
Krolik J. H., 1994, IAU Symposium No. 159: Multi-wavelength continuum emission of AGN, p. 163 - 172
Lauer T. R. & Boroson T. A. 2009, ApJ, 703, 930
Leighly K. M., O'Brien P. T., Edelson R., George I. M., Malkan M. A., Matsuoka M., Mushotzky R. F., Peterson B. M., 1997, ApJ, 483, 767
Lewis K. T. & Eracleous M., 2006, ApJ, 642, 711
Lewis K. T., Eracleous M., Storchi-Bergmann T., 2010, ApJS, 187, 416
Livio M. & Xu C., 1997, ApJ, 478, L63
Maoz D., 1996, in the proceedings of IAU Colloquium 159, Shanghai, June 1996. "Emission Lines in Active Galaxies: New Methods and Techniques", eds. B.M. Peterson, F.-Z. Cheng, and A.S. Wilson (Astronomical Society of the Pacific: San Francisco)
Merritt D. & Ekers R. D., 2002, Science, 297, 1310
Narayan R. & Nityananda R., 1986, ARA&A, 24, 127
O'Brien P.T., Dietrich M., Leighly K., Alloin D., Clavel J., et al., 1998, ApJ, 509, 163
Oke J. B., IN: Superluminal radio sources; Proceedings of the Workshop, Pasadena, CA, Oct. 28-30, 1986 (A88-39751 16-90). Cambridge and New York, Cambridge University Press, 1987, p. 267-272.
Onken C. A., Ferrarese L., Merritt D., Peterson B. M., Pogge R. W., Vestergaard M., Wandel A., 2004, ApJ, 615, 645
Peterson B. M., Balonek T. J., Barker E. S., Bechtold J., Bertram R.,et al., 1991, ApJ, 368, 119
Peterson B. M., Alloin D., Axon D., Balonek T. J., Bertram R., et al., 1992, ApJ, 392, 470
Peterson B. M., 1993, PASP, 105, 247
Peterson B. M., Ali B., Horne K., Bertram R., Lame N. J., Pogge R. W., Wagner R. M., 1993, ApJ, 402, 469
Peterson B. M., Berlind P., Bertram R., Bochkarev N. G., Bond D., et al., 1994, ApJ, 425, 622
Peterson B. M., Wanders I., Horne K., Collier S., 1998, PASP, 110, 660
Peterson B. M., Ferrarese L., Gilbert K. M., Kaspi, S., Malkan M. A., et al., 2004, ApJ, 613, 682
Peterson B. M. & Bentz M. C., 2006, NewAR, 50, 796
Peterson B. M., 2010, Co-Evolution of Central Black Holes and Galaxies, Proceedings of the International Astronomical Union, IAU Symposium, Volume 267, p. 151-160
Pijpers F. P. & Wanders I., 1994, MNRAS, 271, 183
Popovic L. C., 2003, ApJ, 599, 140
Perez E., Penston M. V., Tadhunter C., Mediavilla E., Moles M., 1988, MNRAS, 230, 353
Press W. H., Teukolsky S. A., Vetterling W. T., Flannery B. P., 1992, 'Numerical Recipes in Fortran 77', Second Edition, published by the Press Syndicate of the University of Cambridge, ISBN 0-521-43064-X, P340
Pronik V. I. & Sergeev S. G., 2007, AGN Variability from X-Rays to Radio Waves ASP Conference Series, Vol. 360, Proceedings of the conference held 14-16 June, 2004 at the Crimean Astrophysical Observatory in Crimea, Ukraine. Edited by C. Martin Gaskell, Ian M. McHardy, Bradley M. Peterson and Sergey G. Sergeev. San Francisco: Astronomical Society of the Pacific, 2007., p.231
Sambruna R. M., Reeves J. N., Braito V., Lewis K. T., Eracleous M., et al., 2009, ApJ, 700, 1473
Sergeev S. G., Pronik V. I., Peterson B. M., Sergeeva E. A., Zheng W., 2002, ApJ, 576, 660
Shapovalova A. I., Burenkov A. N., Carrasco L., Chavushyan V. H., Doroshenko V. T., et al., 2001, A&A, 376, 775
Shapovalova A. I., Popovic L. C., Burenkov A. N., Chavushyan V. H., Ilic D., et al., 2010, A&A, 517, 42
Stauffer J., Schild R. & Keel W., 1983, ApJ, 270, 465S
Storchi-Bergmann T., Eracleous M., Livio M., Wilson A. S., Filippenko A. V., Halpern J. P., 1995, ApJ, 443, 617
Storchi-Bergmann T., Eracleous M., Ruiz M. T., Livio M., Wilson A. S., Filippenko A. V., 1997, ApJ, 489, 87
Storchi-Bergmann T., Nemmen da S. R., Eracleous M., Halpern J. P., Wilson A. S., Filippenko A. V., Ruiz M. T., Smith R. C., Nagar N. M., 1997, ApJ, 489, 8
Strateva I. V., Strauss M. A., Hao L., Schlegel D. J., Hall P. B., et al., 2003, AJ, 126, 1720
Tran H. D., 2010, ApJ, 711, 1174
Tremaine S., Gebhardt K., Bender R., Bower, G., Dressler A., et al., 2002, ApJ, 574, 740
van Groningen E. & Wanders I., 1992, PASP, 104, 700
Veilleux S. & Zheng W., 1991, ApJ, 377, 89
Wanders I. & Horne K., 1994, A&A, 289, 76
Weinberg S, 1972, Gravitation and Cosmology. New York: John Wiley and Sons. pp. 185201. ISBN 978-0-471-92567-5
White R. J. & Peterson B. M., 1994, PASP, 106, 876
Winge C., Peterson B. M., Horne K., Pogge R. W., Pastoriza M., Storchi-Bergmann T., 1995, ApJ, 445, 680
Woo J. H. Treu T., Barth A. J., Wright S. A., Walsh J. L., et al., 2010, ApJ, 716, 269
Zhang X. G., Dultzin D., Wang T. G., 2007, MNRAS, 377, 1215
Zhang X. G., Dultzin D., Wang T. G., 2008, MNRAS, 385, 1087
Zheng W., Sulentic J. W., Binette L., 1990, ApJ, 365, 115
Zheng W., Veilleux S., Grandi S. A., 1991, ApJ, 381, 418

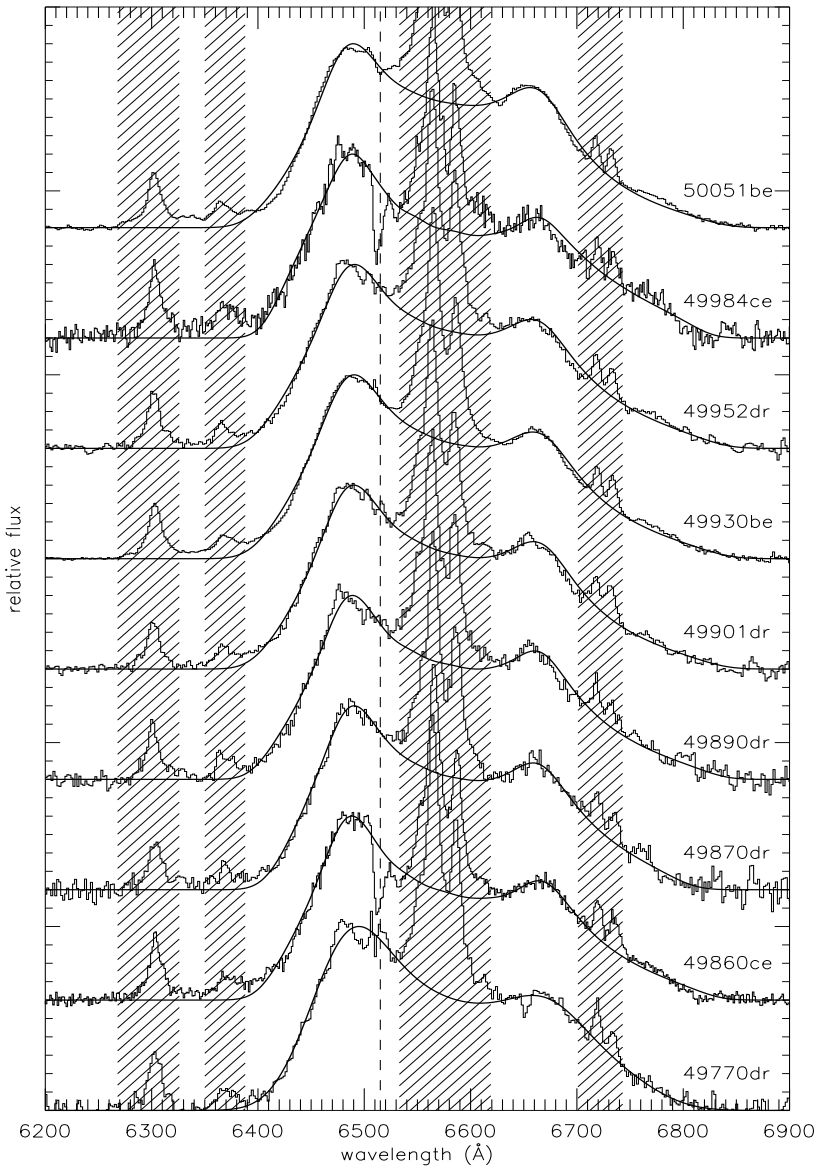

Figure 1. Best fitted results for double-peaked broad Hα in rest wavelength by elliptical accretion disk model. Thin solid line represents the observed spectrum, thick solid line represents the best fitted results for double-peaked broad Hα. The vertical dashed line shows the position for unexpected absorption features around 6500$\mathring{A}$ for two examples marked with '49860ce' and '49984ce'. The observed MJD date of each spectrum is shown in the right side of the figure. Shadow areas represent the ranges for narrow emission lines.

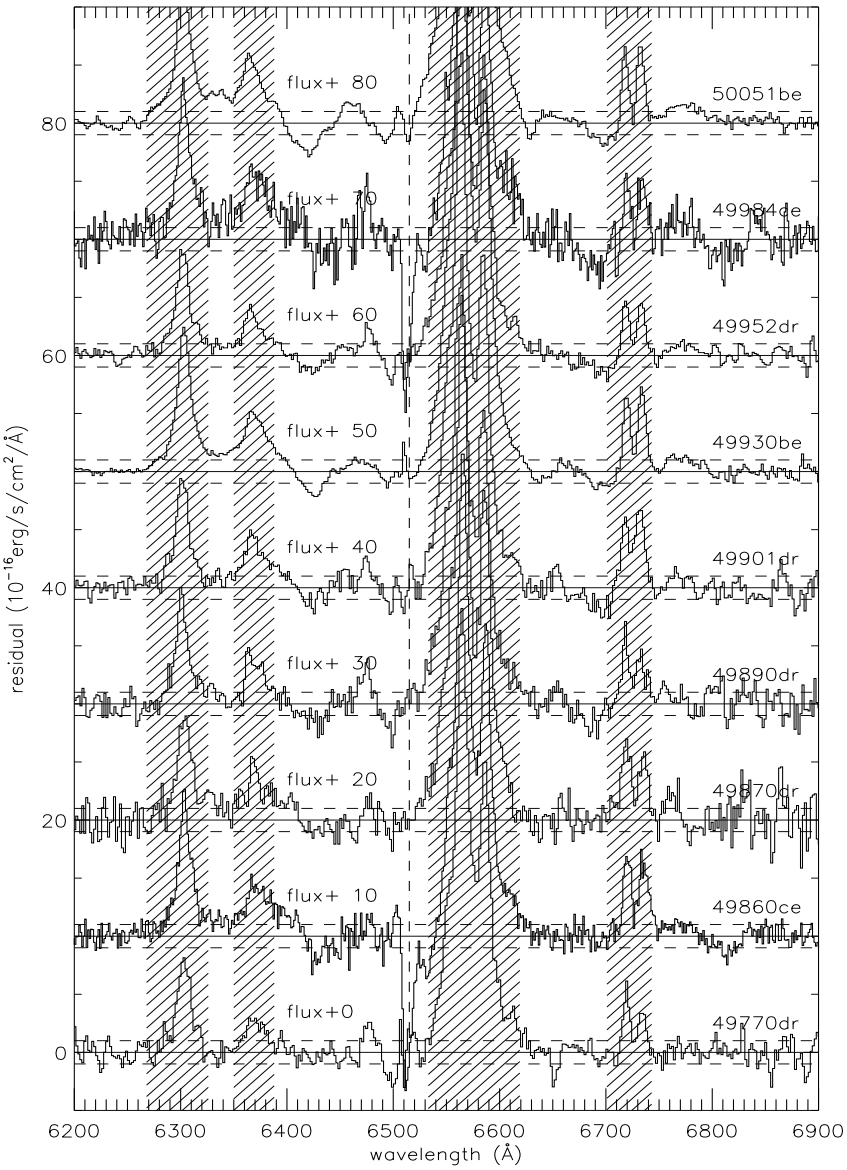

Figure 2. The residuals ($y_{obs} - y_{model}$, observed data minus expected model data) for the shown examples in Figure 1. Shadow areas represent the ranges for narrow emission lines, each double horizontal dashed lines represent the range of $[f_0 - 1, f_0 + 1]$, where $f_0 = 0, 10, 20...80$ representing the zero point for each spectrum are shown as solid horizontal lines in the figure.

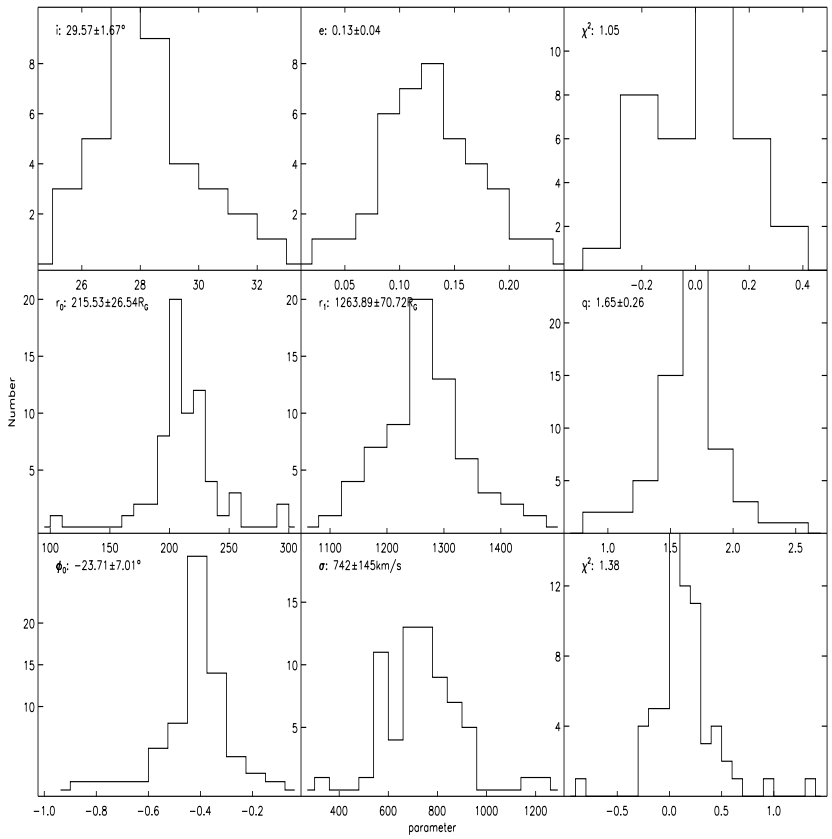

Figure 3. Distributions of the disk parameters of disk-like BLRs for 3C390.3. The top three subfigures show the distributions of eccentricity, inclination angle and the parameter of $\log(\chi^2)$ for the 39 spectra with high quality and without unexpected absorption features around 6500$\mathring{A}$. Then the other six subfigures show the distributions of the other parameters for all the 66 spectra, inner radius r_0, outer radius r_1, emissivity slope q, orientation angle ϕ_0, local broadening velocity σ and the parameter of $\log(\chi^2)$. The mean value of each parameter we accepted is shown in each subfigure.

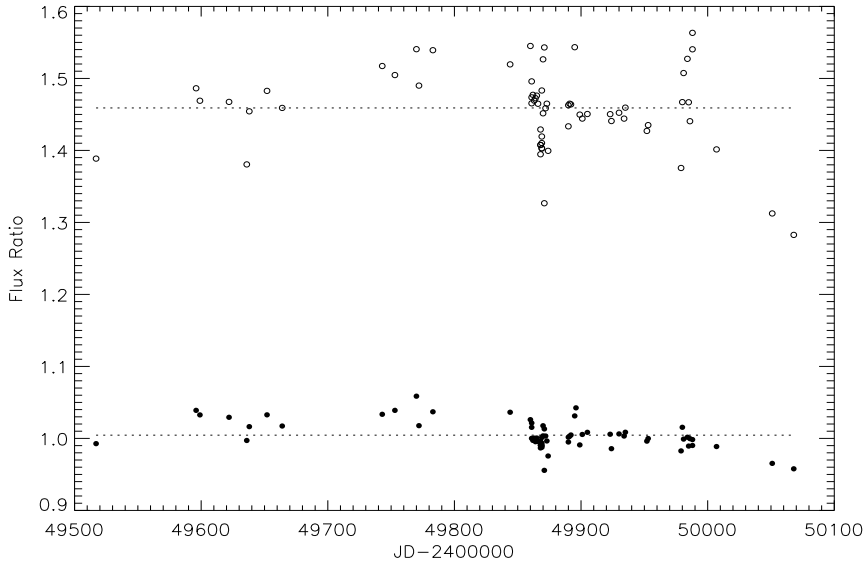

Figure 4. The variations of the flux ratio of blue peak to red peak (shown as open circles), and the flux ratio of blue part to red part of broad Hα (shown as solid circles). The dotted lines represents the mean values of the two kinds of flux ratios.

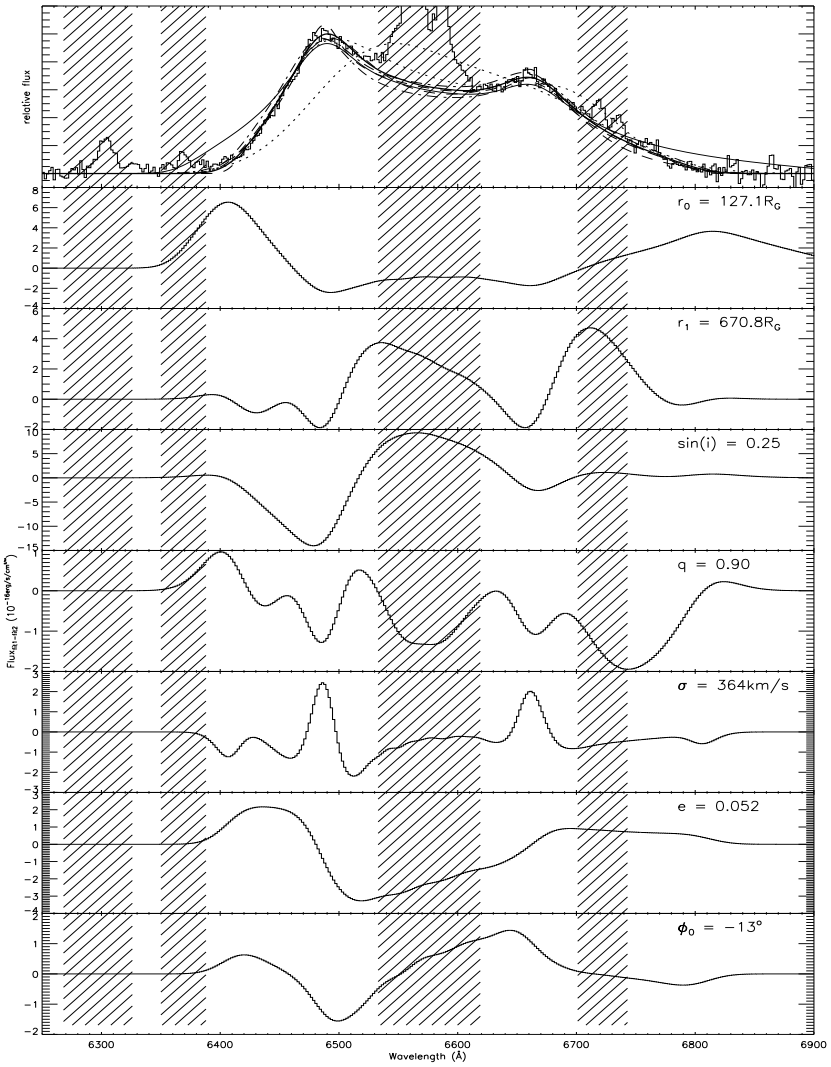

Figure 5. Best fitted results for double-peaked broad Hα with one fixed parameter with half of accepted value for the disk parameter. In the top panel, thin solid line in histogram mode represents the observed line profile marked with '49870dr' in AGN WATCH project, the thick solid line shows the best fitted results with disk parameters having values shown in Figure 3, thin solid line represents the best fitted results with disk parameter $r_0 = 127.1R_G$, thin dotted line represents the best fitted results with disk parameter $r_1 = 670.8R_G$, thick dotted line represents the best fitted results with disk parameter $\sin(i) = 0.25$, thin dashed line represents the best fitted results with disk parameter $q = 0.90$, thick dashed line represents the best fitted results with disk parameter $\sigma = 364km/s$, thin dot-dashed line represents the best fitted results with disk parameter $e = 0.052$, thick dot-dashed line represents the best fitted results with disk parameter $\phi_0 = -13$ in degree. The other seven panels show the corresponding values of $flux_{fit1-fit2}$, where $fit2$ represents the best fitted results with disk parameters shown in Figure 3.

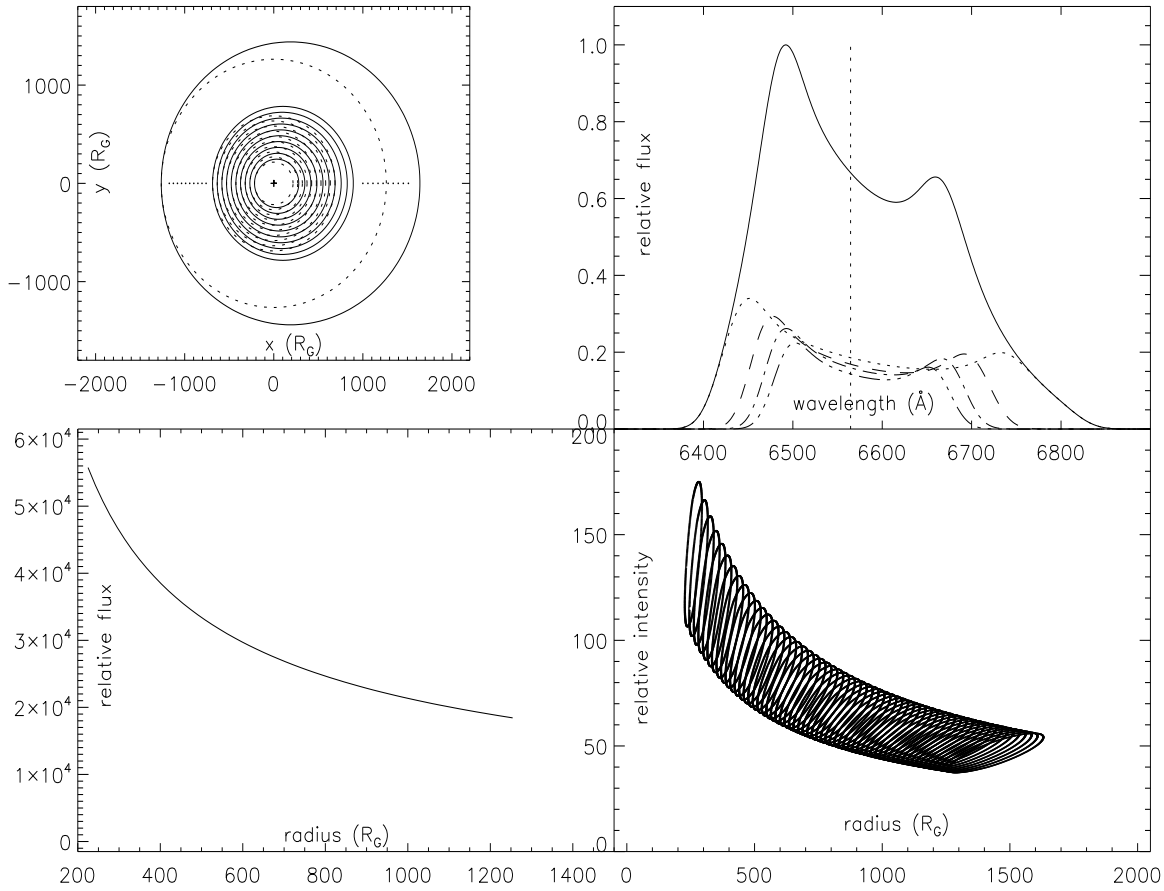

Figure 6. Top left panel shows the toy structures of the elliptical disk-like BLRs of 3C390.3. The solid line represents the elliptical ring with pericenter distance $r_0 \leqslant r_i \leqslant r_1$, the innerest one with pericenter distance of r_0, the outerest one with r_1. The central black hole is located at the origin of the coordinates (one focus point of the elliptical ring). Dotted line represents the sphere surface of ionizing photos at one time. Because the BLRs are elliptical disk-like, thus at one time, the ionizing photos arriving in BLRs DO NOT affect all the tiny clouds located in one elliptical ring. Top right panel show the toy showing of the line intensity of broad Hα from different bins of radius. Solid line represents the observed Hα, dotted line represents the line intensity from $\sim 216R_G$ (the inner boundary) to $\sim 480R_G$, dashed line represents the line intensity from $\sim 480R_G$ to $\sim 740R_G$, dot-dashed line represents the line intensity from $\sim 740R_G$ to $\sim 1000R_G$, double-dot-dashed line represents the line intensity from $\sim 1000R_G$ to $1263R_G$ (the outer boundary). The vertical dotted line represents the center wavelength of Hα, 6564.61Å. Bottom left panel shows the correlation between line intensities from different bins ($F_i(r)$) and the corresponding pericenter distances of the bins. Here the bins are created uniformly, thus $F(r) \propto r^{(\sim(1-q))} \propto r^{(-0.65)}$. Bottom right panel shows the properties of line intensities ($f_{i,j}$) of the 23541 data points in sixty elliptical rings with pericenter distances from r_0 to r_1. The bottom two panels show the properties of Equation (2).

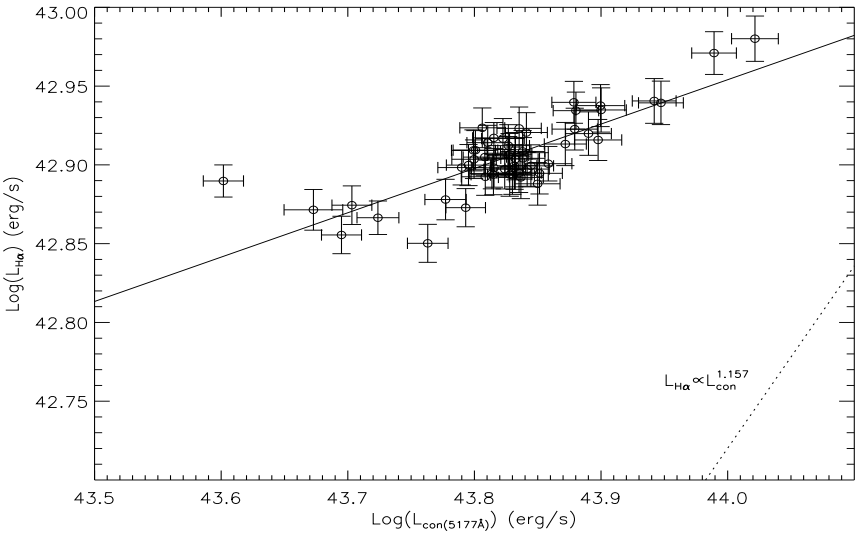

Figure 7. The correlation between luminosity of broad Hα and continuum luminosity at 5177$\mathring{A}$ for 66 observed spectra around 1995. Solid line represents the best fitted result, $L_{H\alpha} \propto (L_{con(5177\mathring{A})})^{0.265}$. The dotted line is the one found by Greene & Ho(2005).

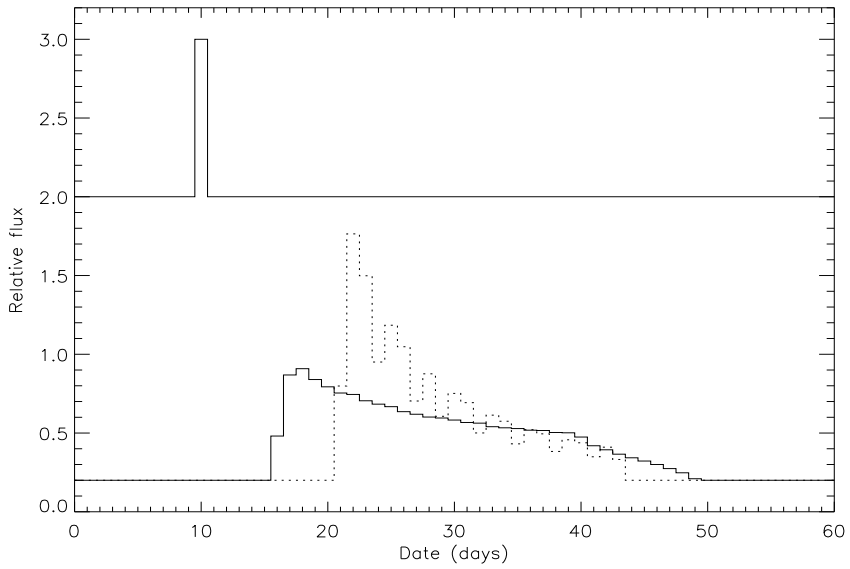

Figure 8. The response output broad Hα based on the input continuum emission described by one delta function under the elliptical disk-like BLRs and circular disk-like BLRs for 3C390.3. The top line shows the continuum emission. The bottom solid line shows the corresponding response output broad Hα under elliptical disk-like BLRs, and dotted line shows the results under circular disk-like BLRs.

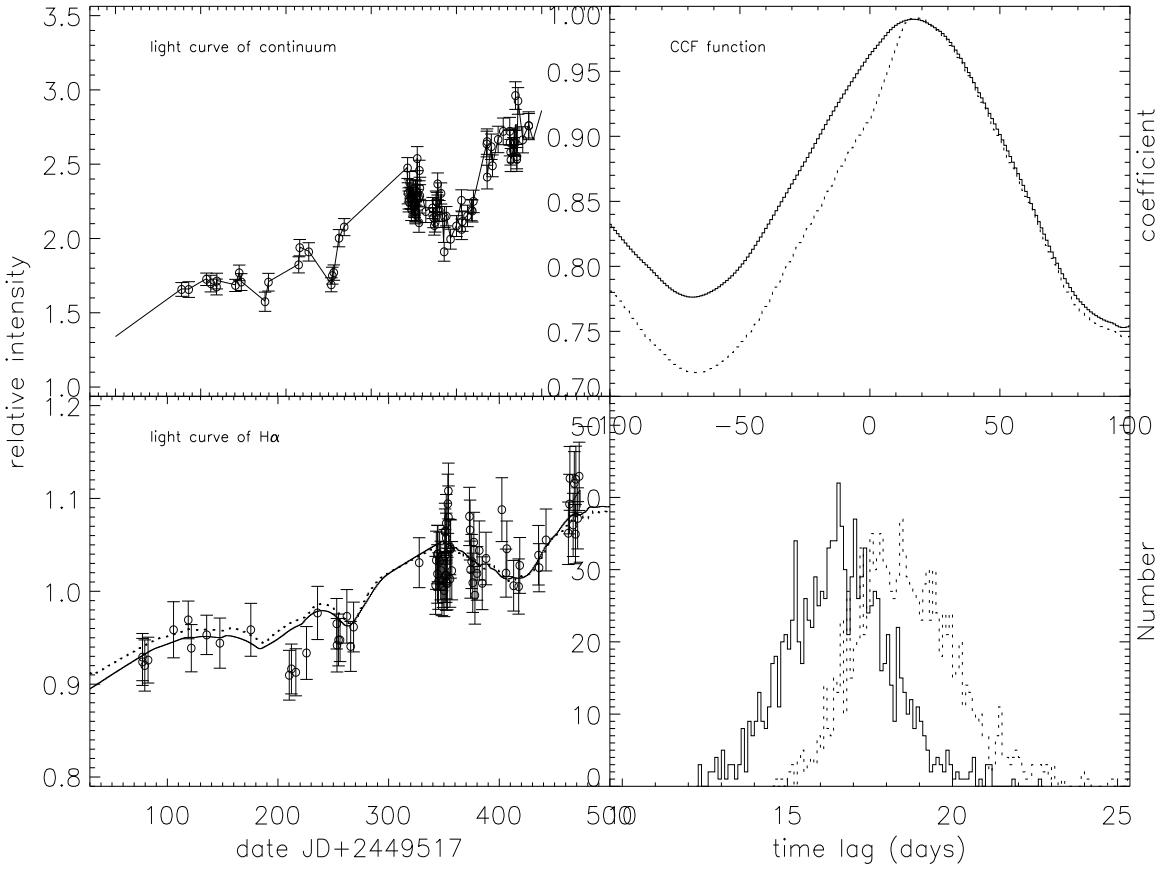

Figure 9. Top left panel shows the light curve of continuum, open circles are the observed data points selected from AGN WATCH, solid line represents the input light curve of continuum with separation of 1day. Bottom left panel shows the light curve of broad Hα, open circles are observed values, solid line represents the output light curve under the elliptical disk-like BLRs, dotted line represents the output light curve under the circular disk model shown in Flohic & Eracleous (2008). Top right panel shows the CCF function (maximum coefficient about 0.99) for observed light-curve of continuum emission and output light curve of broad Hα. Solid line represents the result for elliptical accretion disk model (peak value around 16 days), dotted line shows the result for circular disk model in Flohic & Eracleous (2008) (peak value around 18 days). Bottom right shows the distribution of time lag between observed continuum emission and simulated broad Hα emission by bootstrap method. Solid line is for elliptical disk model, dotted line is for circular disk model in Flohic & Eracleous (2008).

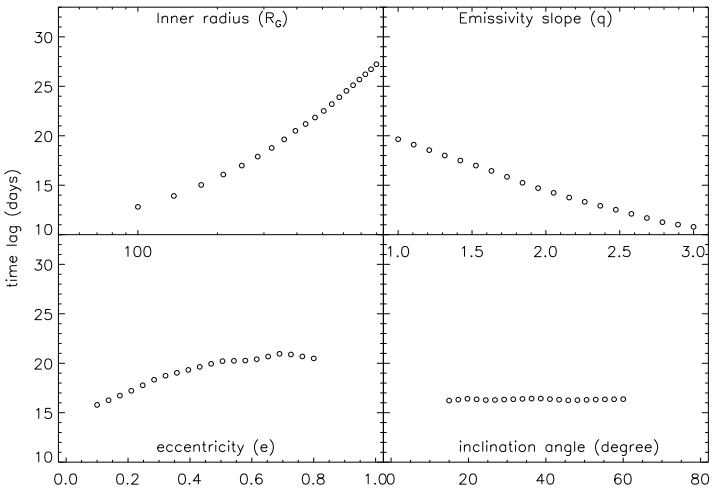

Figure 10. The effects of disk parameters on the theoretically measured size of BLRs. Top-left panel shows the effects of inner radius, top-right panel shows the effects of emissivity power, bottom-left panel shows the effects of eccentricity, bottom-right panel shows the effects of inclination angle.

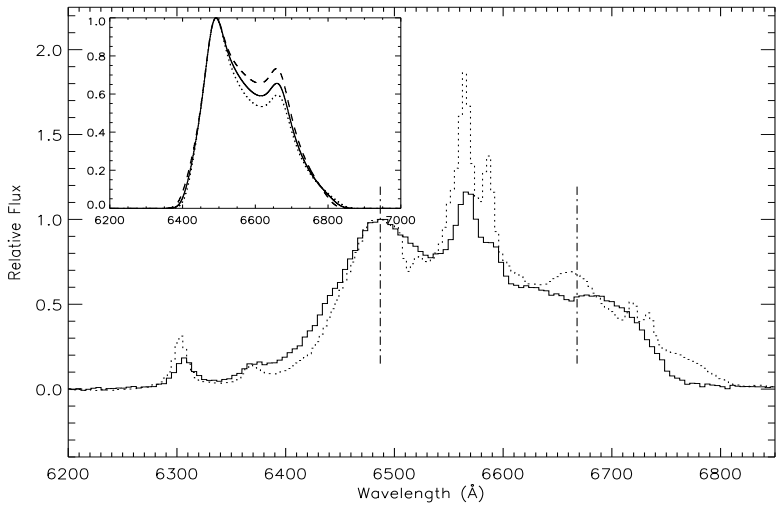

Figure 11. To compare the observed line profile by HST in 2000 and mean observed line profile around 1995. Thin dotted line represents the mean spectrum around 1995 and thick solid line represents the observed line profile by HST in 2000. Two vertical dot-dashed lines mark the positions of red peak and blue peak of double-peaked broad Hα. Top left panel shows the theoretical results. Solid line represents the mean observed double-peaked line profile around 1995, thick dashed line represents the expected line profile around 2000 with clockwise rotating disk-like BLRs, thick dotted line represents the expected line profile around 2000 with anticlockwise rotating disk-like BLRs.